Numerical Analysis of Kinetic Rate Constants Derived from Stochastic Computer Simulation

Peiru Wu and Victoria L. McGuffin
Dept. of Chemistry and Center for Fundamental Materials Research, Michigan State University, East Lansing, MI 48824

A numerical approach has been developed to determine the individual rate constants (k_{f-s} and k_{s-f}), as well as the equilibrium constant from the ratio of the rate constants (k_{f-s}/k_{s-f}), by using stochastic simulation. This approach is illustrated for simulations of the absorption (partition) process between homogeneous fluid and surface phases under diffusion-limited conditions. A pair of regression methods is derived from the chemical system with the initial distribution of molecules entirely in either the fluid or surface phase. These two methods are complementary in determining the rate constants for distribution coefficients that are lower or higher than unity, respectively. A standard exponential (two-parameter) regression equation is compared with a biexponential (four-parameter) equation, which provides for inherent correction of numerical error. The effects of the number of molecules, as well as the time increment and range, are examined in detail. This provides guidance to optimize the computational parameters of the simulation. The proposed approach has been successfully applied for distribution coefficients ranging from 0.01 to 100.0, yielding individual rate constants k_{f-s} and k_{s-f} with $\pm$ 0.84% and $\pm$ 0.57% average relative standard deviation, and the ratio of the rate constants with $\pm$ 1.04% average relative standard deviation and $\pm$ 1.14% average relative error.

Introduction

In recent years, stochastic or Monte Carlo simulation methods have been employed to study a wide variety of problems in chemistry and chemical engineering. One advantage of such methods is that they deal with the behavior of individual species (such as atoms, molecules, and particles), rather than the bulk or average behavior of statistical ensembles. By monitoring the positions or trajectories of these individual species in three-dimensional (3-D) space, a direct and detailed interpretation of physical and chemical phenomena is possible. These simulation methods are a powerful and versatile means to model complex systems, which can provide the connection between molecular-level models (such as *ab initio* quantum mechanical or molecular dynamics calculations) and classical theoretical models or experiments.

Stochastic simulations have been widely used to study adsorption, desorption, and associated processes as a function of the surface structure and properties. From these simulations, the adsorption isotherms (Patrykiejew and Jaroniec, 1984; Patrykiejew, 1992), phase transitions (Patrykiejew, 1981, 1982), and thermodynamic properties (Patrykiejew, 1983, 1988) have been calculated for adsorbates on homogeneous surfaces, as well as on random and organized heterogeneous surfaces. In addition, the fractional surface coverage and phase diagrams have been determined for binary mixtures of adsorbates (Patrykiejew, 1987, 1988). For adsorbates that are partially or fully mobile, the stochastic simulation method has enabled the study of aggregation or island formation (Binder, 1986, 1987), as well as the concomitant effects upon the rates of desorption (Gupta and Hirtzel, 1984; Hood et al., 1985) and surface reactions (Silverberg et al., 1985; Silverberg and Ben-Shaul, 1987; Stiles and Metiu, 1986; Kang et al., 1990).

Stochastic simulations have also been applied to characterize diffusion phenomena in bulk solution (Kawasaki, 1966a,b,c) as well as at homogeneous and heterogeneous surfaces (Kang and Weinberg, 1989, 1992). The surface diffusion coefficients have been estimated as a function of the adsor-

Correspondence concerning this article should be addressed to V. L. McGuffin.

bate–adsorbate and adsorbate–surface interaction energies (Bowker and King, 1978a,b; Murch, 1980; Kutner et al., 1982, 1983; Sadiq and Binder, 1983; Mak et al., 1988; Ray and Baetzold, 1990). In addition, the transition between ordinary and Knudsen diffusion has been studied in porous media consisting of randomly overlapping fibers as well as parallel, nonoverlapping, or partially overlapping fibers (Tomadakis and Sotirchos, 1991a,b, 1993a,b). From these simulations, the porosity, internal surface area, and accessibility of the fibrous structures have been calculated, together with the effective diffusion coefficients (Burganos and Sotirchos, 1988, 1989).

In addition to these studies of stationary systems, stochastic simulations have also been used to characterize systems with convective transport (Celenligil et al., 1989; Sotirchos, 1989). Chemical reactions performed in homogeneous solutions have been modeled under laminar flow conditions in a cylindrical tube (Betteridge et al., 1984; Wentzell et al., 1993). Laminar flow conditions have also been modeled in thin, rectangular channels which exhibited an unusual Coriolis-induced secondary flow (Schure, 1988; Schure and Weeratunga, 1991). More recently, the stochastic method has been used to simulate adsorption and absorption at the wall of cylindrical tubes under both laminar (McGuffin and Wu, 1996) and electroosmotic (Schure and Lenhoff, 1993; McGuffin et al., 1995; Hopkins and McGuffin, 1998) flow conditions.

In these prior studies, stochastic simulation methods have primarily been used to elucidate the steady-state or equilibrium properties of the model system. However, if the simulation is judiciously designed so that it accurately represents the time evolution of the model system, then it may also be utilized to investigate kinetic phenomena (Fichthorn and Weinberg, 1991; Kang and Weinberg, 1992). This approach may be used to identify and characterize the rate-limiting processes in complex mass-transport systems, such as those used for catalysis or separations. A deeper understanding of kinetic phenomena is necessary in order to increase the speed of such systems with a minimal sacrifice in yield and efficiency. The purpose of the present work is to develop a reliable approach to derive kinetic rate constants from stochastic simulations and to evaluate their statistical accuracy and precision.

Computer Simulation

A 3-D stochastic computer simulation of transport processes in heterogeneous systems has been developed in the FORTRAN 90 programming language and optimized on an IBM RS/6000 Model 580 computer. The input parameters required for this simulation may be divided into three general categories, as summarized in Table 1. The system parameters describe properties of the fluid and surface, as well as the spatial dimensions of the system to be simulated. The molecular parameters describe attributes of the molecules, and the computational parameters describe certain constraints that are required for the simulation. To initialize the simulation, the molecules are distributed in a statistically random manner entirely in either the fluid or surface phase. The simulation program, shown in the flowchart in Figure 1, incorporates algorithms for the mass-transport processes of diffusion, convection by laminar and electroosmotic flow, and surface interaction by absorption and adsorption mechanisms

Table 1. Variable Simulation Parameters and Typical Values Used in the Present Work

System Parameters:	Symbol	Value
Radius of fluid phase	R	20.0×10^{-4} cm
Length of fluid phase	L	100 cm
Viscosity of fluid phase	η	
Dielectric constant of fluid phase	ϵ	
Ionic strength of fluid phase	I	
Mean linear velocity of fluid phase	v_0	0 cm·s^{-1}
Depth of surface phase	d_s	4.49×10^{-4} cm
Zeta potential of surface phase	ζ	
Voltage	V	
Pressure	P	
Temperature	T_0	298 K
Molecular Parameters:		
Diffusion coefficient	D_f	1.0×10^{-5} cm^2·s^{-1}
	D_s	1.0×10^{-6} cm^2·s^{-1}
Distribution coefficient	K	0.01–500
Adsorption energy	E	
Mobility	μ	
Charge	z_i	
Computational Parameters:		
Number of molecules	N	$1.0\times10^{-3}-1.0\times10^{5}$
Molecular-frame coordinates	ρ, ϕ, θ	
Global-frame coordinates		
cylindrical	r, θ, z	
Cartesian	x, y, z	
Time increment	t	$5.0\times10^{-6}-5.0\times10^{-3}$
Total simulation time	T	0.05–5.0 s

(McGuffin et al., 1995; McGuffin and Wu, 1996; McGuffin and Hopkins, 1998). The selected processes are repeated for each molecule at each time increment (t) until the total simulation time (T) is reached.

In the present study, we simulate a simple absorption (partition) mechanism between a homogeneous fluid phase that is in contact with a permeable and homogeneous surface phase. These simulations are representative of several types of practical systems, such as an electrochemical or mass sensor overcoated with a thin polymer film, or a separation based on a membrane or chromatographic column. In order to simulate the absorption mechanism for solute molecules in such systems, the algorithms for the processes of diffusion and surface interaction are required. Molecular diffusion is simulated by using a 3-D extension of the Einstein-Smoluchowski equation (Einstein, 1905; Feller, 1950; Reid et al., 1977). The radial distance ρ traveled by a molecule during the time increment t is given by

$$\rho = (6D_{f,s}t)^{1/2} \tag{1}$$

where $D_{f,s}$ is the diffusion coefficient in the fluid or surface phase, as appropriate. The direction of travel is subsequently randomized through the spherical coordinate angles (ϕ, θ). Finally, the coordinate increments in the molecular frame are used to calculate the new molecular position in the global coordinate frame. This algorithm has been validated for diffusion coefficients ranging from 10^{-1} to 10^{-8} cm^2·s^{-1}, with average relative errors in distance and variance of $\pm0.32\%$ and $\pm2.96\%$, respectively (McGuffin and Wu, 1996).

For surface interaction by an absorption process, the probability of transport between the fluid and surface phases is derived from the long-time behavior of a single molecule,

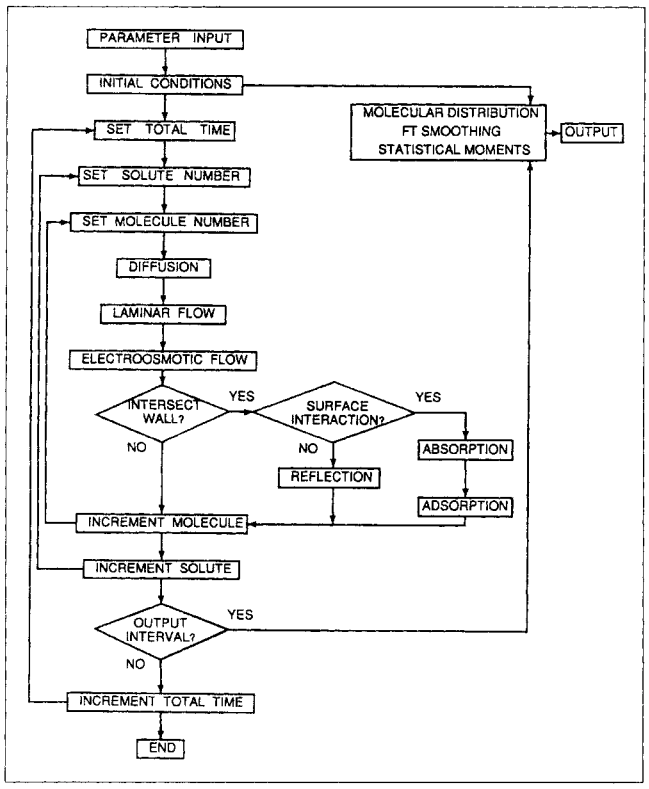

Figure 1. Flowchart of the computer simulation program.

rather than from the bulk behavior of an ensemble of molecules. Consider a small incremental volume of the fluid and surface phases at the interface wherein the probability of the molecule striking the interface approaches unity in each time increment. These incremental volumes may be expressed as $dV_f = (2D_f t)^{1/2}\, dA$ and $dV_s = (2D_s t)^{1/2}\, dA$, where dA is the incremental surface area and t is the time increment. Now consider a total time $T = [1 + K(dV_s/dV_f)]t = [1 + K(D_s/D_f)^{1/2}]t$. Of this total time, the molecule must spend a time $T_f = t$ in the fluid phase and $T_s = K(D_s/D_f)^{1/2}t$ in the surface phase in order to satisfy the expected long-time behavior. By substitution, the probabilities of transport between the fluid and surface phases can be expressed as

$$\frac{P_{f-s}}{P_{s-f}} = \frac{T_s}{T_f} = K\left(\frac{D_s}{D_f}\right)^{1/2} \tag{2}$$

To derive expressions for the individual probabilities P_{f-s} and P_{s-f}, we can consider two limiting cases. First, if $K(D_s/D_f)^{1/2} \gg 1$ and the molecule is in the fluid phase (having already spent one time increment there and having satisfied the requirement that $T_f = t$), then it must be transferred to the surface phase. Under these conditions

$$P_{f-s} = 1 \quad \text{and} \quad P_{s-f} = K^{-1}\left(\frac{D_f}{D_s}\right)^{1/2} \tag{3a}$$

Similarly, if $K(D_s/D_f)^{1/2} \ll 1$ and the molecule is in the surface phase, then it must be transferred to the fluid phase. Under these conditions

$$P_{f-s} = K\left(\frac{D_s}{D_f}\right)^{1/2} \quad \text{and} \quad P_{s-f} = 1 \tag{3b}$$

It is noteworthy that the product $K(D_s/D_f)^{1/2}$, which is intrinsically related to the probabilities P_{f-s} and P_{s-f} for transfer of a single molecule, has recently been identified as the nonequilibrium partition constant (Morita, 1996; Barzykin and Tachiya, 1998). When a molecule encounters the fluid–surface interface during the simulation, a random number between zero and one is selected. This random number is compared with the probability P_{f-s} or P_{s-f} if the molecule is in the fluid or surface phase, respectively, as given by Eq. 3a if $K(D_s/D_f)^{1/2} \geq 1$ or by Eq. 3b if $K(D_s/D_f)^{1/2} \leq 1$. If the random number is less than or equal to the probability, the molecule is transferred along the initial trajectory across the interface to the opposite phase. Otherwise, the molecule remains in the same phase and undergoes an elastic collision at the interface. Similarly, when a molecule encounters a spatial boundary of the system, an elastic collision is performed. This algorithm has been validated for distribution coefficients ranging from 0.01 to 100.0, with average relative errors in distance and variance of $\pm 0.55\%$ and $\pm 4.02\%$, respectively (McGuffin and Wu, 1996).

In the present study, stochastic simulations are performed for an absorption system with constant radius of the fluid phase ($R = 20.0 \times 10^{-4}$ cm), depth of the surface phase ($d_s = 4.49 \times 10^{-4}$ cm), as well as diffusion coefficients of the molecule in the fluid and surface phases ($D_f = 1.0 \times 10^{-5}$ cm$^2 \cdot$s^{-1} and $D_s = 1.0 \times 10^{-6}$ cm$^2 \cdot$s^{-1}). These simulations are used to develop and, subsequently, to validate numerical methods that characterize the kinetic and equilibrium behavior of the system.

Numerical Approach to Determine Rate Constants

In the absorption mechanism, the solute X is distributed between the homogeneous fluid and surface phases by a reversible reaction

$$X_f \underset{k_{s-f}}{\overset{k_{f-s}}{\rightleftarrows}} X_s \tag{4}$$

where k_{f-s} and k_{s-f} are the first-order rate constants. When the system is in equilibrium, the ratio of the number of solute molecules in the fluid phase ($\tilde{N}_f$) and surface phase ($\tilde{N}_s$) defines the distribution coefficient (K)

$$\frac{KV_s}{V_f} = \frac{\tilde{N}_s}{\tilde{N}_f} = \frac{k_{f-s}}{k_{s-f}} \tag{5}$$

which is adjusted for the relative volumes of the fluid phase ($V_f = \pi R^2 L$) and the surface phase ($V_s = \pi(d_s^2 + 2Rd_s)\, L$).

Prior to equilibrium, however, the distribution of solute molecules can be described by a kinetic model of reversible

reactions (Benson, 1960; Steinfeld et al., 1989). Under these conditions, the net rate of change in the number of molecules in the fluid and surface phases is governed by a system of ordinary differential equations (ODE)

$$\begin{cases} \dfrac{dN_f}{dT} = -k_{f-s}N_f + k_{s-f}N_s & (6a) \\ \dfrac{dN_s}{dT} = k_{f-s}N_f - k_{s-f}N_s & (6b) \end{cases}$$

Two important initial conditions are associated with this ODE system:

(i) all molecules initially reside in the fluid phase, that is,

$$N_f = N \quad \text{and} \quad N_s = 0 \quad \text{at} \quad T = 0 \tag{7}$$

(ii) all molecules initially reside in the surface phase, that is,

$$N_f = 0 \quad \text{and} \quad N_s = N \quad \text{at} \quad T = 0 \tag{8}$$

where N is the total number of molecules. As shown in Figure 2, the chemical system will eventually reach the equilibrium state from either of these two initial conditions, so that the ratio of the number of molecules in the fluid and surface phases remains constant as time approaches infinity.

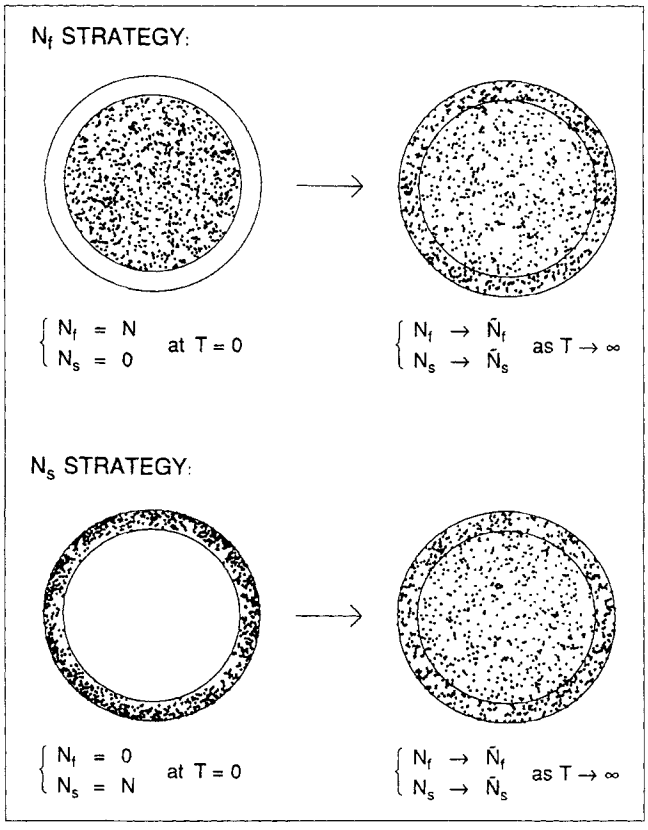

Figure 2. Relationship between the two initial conditions associated with the ODE system (Eqs. 6a and 6b) and the equilibrium state.

Equations 6 and 7 (or, alternatively, Eqs. 6 and 8) may be rewritten as follows

$$\begin{cases} \dfrac{d\boldsymbol{N}(T)}{dT} = \boldsymbol{A}\boldsymbol{N}(T) & (9a) \\ \boldsymbol{N}(0) = \boldsymbol{N}_0 & (9b) \end{cases}$$

where

$$\boldsymbol{N}(T) = \begin{pmatrix} N_f \\ N_s \end{pmatrix} \quad \text{and} \quad \boldsymbol{A} = \begin{pmatrix} -k_{f-s} & k_{s-f} \\ k_{f-s} & -k_{s-f} \end{pmatrix} \tag{10}$$

For the initial condition (i)

$$\boldsymbol{N}_0 = \begin{pmatrix} N \\ 0 \end{pmatrix} \tag{11a}$$

For the initial condition (ii)

$$\boldsymbol{N}_0 = \begin{pmatrix} 0 \\ N \end{pmatrix} \tag{11b}$$

By the standard ODE theory, the solution of Eq. 9 is given by

$$\boldsymbol{N}(T) = \boldsymbol{c}_1 \exp(\lambda_1 T) + \boldsymbol{c}_2 \exp(\lambda_2 T) \tag{12}$$

where $\boldsymbol{c}_1$ and $\boldsymbol{c}_2$ are eigenvectors of the matrix $\boldsymbol{A}$ associated with its eigenvalues λ_1 and λ_2, respectively,

$$\lambda_1 = 0 \quad \text{and} \quad \lambda_2 = -(k_{f-s} + k_{s-f}) \tag{13}$$

which can be determined uniquely by the initial condition in Eq. 11a or 11b. For the initial condition (i)

$$\boldsymbol{c}_1 = \frac{N}{k_{f-s} + k_{s-f}} \begin{pmatrix} k_{s-f} \\ k_{f-s} \end{pmatrix} \quad \text{and} \quad \boldsymbol{c}_2 = \frac{N}{k_{f-s} + k_{s-f}} \begin{pmatrix} k_{f-s} \\ -k_{f-s} \end{pmatrix} \tag{14}$$

and

$$\begin{pmatrix} N_f \\ N_s \end{pmatrix} = \frac{N}{k_{f-s} + k_{s-f}} \times \begin{cases} k_{s-f} + k_{f-s}\exp[-(k_{f-s} + k_{s-f})T] & (15a) \\ k_{f-s} - k_{f-s}\exp[-(k_{f-s} + k_{s-f})T] & (15b) \end{cases}$$

Similarly, for the initial condition (ii)

$$\boldsymbol{c}_1 = \frac{N}{k_{f-s} + k_{s-f}} \begin{pmatrix} k_{s-f} \\ k_{f-s} \end{pmatrix} \quad \text{and} \quad \boldsymbol{c}_2 = \frac{N}{k_{f-s} + k_{s-f}} \begin{pmatrix} -k_{s-f} \\ k_{s-f} \end{pmatrix} \tag{16}$$

and

$$\begin{pmatrix} N_f \\ N_s \end{pmatrix} = \frac{N}{k_{f-s}+k_{s-f}} \times \begin{Bmatrix} k_{s-f} - k_{s-f}\exp[-(k_{f-s}+k_{s-f})T] \\ k_{f-s} + k_{s-f}\exp[-(k_{f-s}+k_{s-f})T] \end{Bmatrix} \quad \begin{matrix} (17a) \\ (17b) \end{matrix}$$

From Eqs. 15a and 15b or 17a and 17b, it is readily apparent that

$$\tilde{N}_f = \lim_{T\to\infty} N_f = \frac{k_{s-f}N}{k_{f-s}+k_{s-f}} \tag{18a}$$

and

$$\tilde{N}_s = \lim_{T\to\infty} N_s = \frac{k_{f-s}N}{k_{f-s}+k_{s-f}} \tag{18b}$$

where $\tilde{N}_f$ and $\tilde{N}_s$ are constant. The ratio $\tilde{N}_s/\tilde{N}_f$ represents the ratio of the number of molecules in surface and fluid phases under the equilibrium definition according to Eq. 5, and is equal to the ratio of the rate constants k_{f-s}/k_{s-f} under the kinetic definition.

It should be noted that for any given matrix A and initial condition N_0, the solution of the ODE system in Eq. 9 is determined uniquely by using Eqs. 12 to 14 or Eqs. 12, 13, and 16 and, hence, so are N_f and N_s by using Eqs. 15a and 15b or 17a and 17b. In other words, if the rate constants k_{f-s} and k_{s-f} are known, then the distribution of molecules in the fluid and surface phases can be exactly calculated as a function of time. However, for a given set of data (such as N_f or N_s vs. T), it is only possible to solve numerically for the rate constants k_{f-s} and k_{s-f} from Eqs. 15a and 15b or 17a and 17b by a nonlinear regression approach. This mathematical consequence remains true no matter how abundant or how accurate the data may be. As the estimation of k_{f-s} and k_{s-f} from the data is a common and important goal of both simulation and experimental studies, it is necessary to develop a reliable strategy for the nonlinear regression approach.

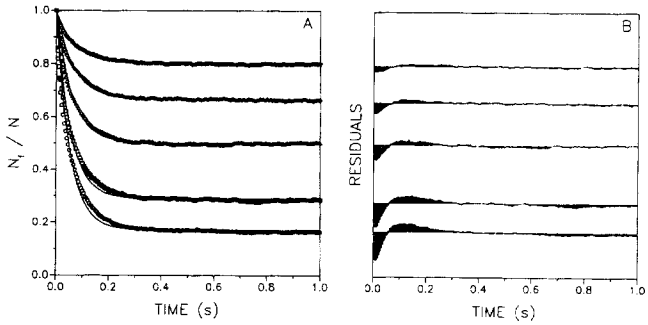

Figure 3. Kinetic evolution of the absorption process by monitoring the relative number of molecules in the fluid phase as a function of simulation time.

Simulation conditions: $N = 1.0\times10^4$; $t = 5.0\times10^{-5}$ s; $R = 20.0\times10^{-4}$ cm; $d_s = 4.49\times10^{-4}$ cm; $D_f = 1.0\times10^{-5}$ cm$^2\cdot$s^{-1}; $D_s = 1.0\times10^{-6}$ cm$^2\cdot$s^{-1}; $K = 0.5$ (∇), 1.0 (◇), 2.0 (△), 5.0 (□), 10.0 (○). (—) Nonlinear regression analysis according to Eq. 15a, together with the associated residuals.

Nonlinear regression strategies

Consider the case wherein all molecules reside initially in the fluid phase, and the number of molecules remaining in the fluid phase is monitored as a function of time. For the set of simulation data (T, N_f), the rate constants k_{f-s} and k_{s-f} can be determined by applying nonlinear regression with an exponential (two-parameter) fitting according to Eq. 15a. An example of the two-parameter fitting strategy is illustrated in Figure 3. From nonlinear regression analysis of the simulation data in the center curve ($K = 2.0$, $V_f/V_s = 2.0$), the rate constants k_{f-s} and k_{s-f} are determined to be 8.36 ± 0.11 s^{-1} and 8.40 ± 0.12 s^{-1}, respectively. Although the probability of molecular transfer from fluid to surface phase ($P_{f-s} = 0.63$) is less than that from surface to fluid phase ($P_{s-f} = 1.00$) according to Eq. 3b, the rate constants are approximately equal because of the commensurately larger volume of the fluid phase. The ratio of these rate constants ($k_{f-s}/k_{s-f} = 0.99\pm0.02$) is in accord with the ratio of the number of molecules in the surface and fluid phases at equilibrium ($\tilde{N}_s/\tilde{N}_f = 1.00$

Table 2. Kinetic Rate Constants k_{f-s} and k_{s-f} Determined by Nonlinear Regression with Two-Parameter Fitting in Eq. 15a for the Case of $N = 1.0\times10^4$ and $t = 5.0\times10^{-5}$ s

K	V_f/V_s	k_{f-s} (s^{-1})	k_{s-f} (s^{-1})	k_{f-s}/k_{s-f}	Error (%)	$\tilde{N}_s/\tilde{N}_f$	Error (%)
500.0	2.0	20.32±0.32	0.20±0.04	100.88±19.47	−59.65	254.02±20.39	1.61
200.0	2.0	20.38±0.32	0.33±0.04	61.97±12.16	−38.03	98.45±7.81	−1.55
100.0	2.0	20.05±0.30	0.53±0.04	38.07±2.92	−23.87	49.08±1.53	−1.85
50.0	2.0	19.28±0.29	0.88±0.04	21.94±1.08	−12.24	25.56±0.60	2.23
20.0	2.0	17.84±0.27	1.90±0.05	9.38±0.29	−6.21	10.04±0.13	0.41
10.0	2.0	16.15±0.24	3.34±0.07	4.83±0.12	−3.34	5.08±0.06	1.55
5.0	2.0	13.19±0.20	5.39±0.10	2.45±0.06	−2.11	2.53±0.03	1.13
2.0	2.0	8.36±0.11	8.40±0.12	0.99±0.02	−0.51	1.00±0.009	0.32
1.0	2.0	5.09±0.06	10.22±0.14	0.50±0.009	−0.41	0.50±0.004	0.47
0.5	2.0	2.94±0.04	11.79±0.17	0.25±0.005	−0.22	0.25±0.002	1.14
0.2	2.0	1.30±0.02	13.19±0.20	0.099±0.002	−1.12	0.098±0.002	−1.66
0.1	2.0	0.67±0.009	13.64±0.20	0.049±0.001	−2.08	0.049±0.001	−1.40
0.05	2.0	0.36±0.007	14.20±0.28	0.025±0.0007	0.37	0.025±0.0006	−1.00
0.02	2.0	0.15±0.005	15.46±0.50	0.010±0.0005	0.12	0.010±0.0006	−0.48
0.01	2.0	0.08±0.004	16.62±0.82	0.005±0.0003	−6.46	0.005±0.0003	−8.58

± 0.009). Moreover, both the kinetic and equilibrium descriptions of the molecular distribution show excellent agreement with the theoretically expected value ($K\ (V_s/V_f) = 1.00$) from Eq. 5. Upon substitution of these rate constants into Eq. 6, the principle of detailed balance reveals that each molecule is transferred from fluid to surface phase an average of 4.175 times per second, and from surface to fluid phase an average of 4.207 times per second at equilibrium.

The simulation results with varying distribution coefficient, but all other conditions remaining constant, are also included in Figure 3. For a rapidly reversible absorption mechanism, these rate constants represent diffusion-limited conditions: that is, the rate constant k_{f-s} is controlled by diffusional mass transport in the fluid phase and the rate constant k_{s-f} by that in the surface phase. Under these conditions, Figure 3A illustrates that the number of molecules in the fluid phase reaches $1-1/e$ of its steady-state value after a characteristic time τ of approximately 0.060 s and that equilibration is virtually complete after 5τ or 0.30 s for all cases. Figure 3B shows that the residuals of the regression analysis are small and behave consistently with varying distribution coefficient, which verifies that the classical exponential fitting approach works reasonably well. This approach has been used to determine the rate constants as a function of distribution coefficient in the range from 0.01 to 500.0, as summarized in Table 2. It is evident that this regression strategy is broadly applicable, so that the individual rate constants and their ratio can be calculated with reasonably good precision and accuracy.

Upon more detailed inspection of Figure 3, however, there appears to be a systematic deviation of the residuals as a function of time, with negative error prior to time τ and positive error thereafter. In addition, Table 2 indicates that the numerical accuracy for the ratio of the rate constants (k_{f-s}/k_{s-f}) becomes progressively worse with increasing distribution coefficient whereas the ratio of the number of molecules ($\tilde{N}_s/\tilde{N}_f$) does not. These results suggest that there is a systematic error in the numerical determination of k_{f-s} and k_{s-f}. This error may arise from several sources when approximating the ODE equation:

(I) Constant or additive error in the number of molecules (ϵ_N^a)

(II) Proportional or multiplicative error in the number of molecules (ϵ_N^m)

(III) Time-dependent error (ϵ_T)

Accordingly, Eqs. 6a and 6b may be replaced by the following three revised ODE systems

$$\text{(I)}\quad \begin{cases} \dfrac{dN_f}{dT} = -(k_{f-s} + \epsilon_{Nf}^a)N_f + (k_{s-f} + \epsilon_{Ns}^a)N_s & (19a) \\ \dfrac{dN_s}{dT} = (k_{f-s} + \epsilon_{Nf}^a)N_f - (k_{s-f} + \epsilon_{Ns}^a)N_s & (19b) \end{cases}$$

$$\text{(II)}\quad \begin{cases} \dfrac{dN_f}{dT} = -(1 + \epsilon_{Nf}^m)k_{f-s}N_f + (1 + \epsilon_{Ns}^m)k_{s-f}N_s & (20a) \\ \dfrac{dN_s}{dT} = (1 + \epsilon_{Nf}^m)k_{f-s}N_f - (1 + \epsilon_{Ns}^m)k_{s-f}N_s & (20b) \end{cases}$$

$$\text{(III)}\quad \begin{cases} \dfrac{dN_f}{dT} = -k_{f-s}N_f + k_{s-f}N_s + \epsilon_{Tf} & (21a) \\ \dfrac{dN_s}{dT} = k_{f-s}N_f - k_{s-f}N_s + \epsilon_{Ts} & (21b) \end{cases}$$

where the subscripts f and s denote the fluid and surface phases, respectively. Similarly, Eqs. 19 to 21 can be rewritten as

$$\text{(I)}\quad \begin{cases} \dfrac{dN_{\rm I}(T)}{dT} = A_{\rm I}N_{\rm I}(T) & (22a) \\ A_{\rm I} = \begin{pmatrix} -(k_{f-s} + \epsilon_{Nf}^a) & k_{s-f} + \epsilon_{Ns}^a \\ k_{f-s} + \epsilon_{Nf}^a & -(k_{s-f} + \epsilon_{Ns}^a) \end{pmatrix} & (22b) \end{cases}$$

$$\text{(II)}\quad \begin{cases} \dfrac{dN_{\rm II}(T)}{dT} = A_{\rm II}N_{\rm II}(T) & (23a) \\ A_{\rm II} = \begin{pmatrix} -(1 + \epsilon_{Nf}^m)k_{f-s} & (1 + \epsilon_{Ns}^m)k_{s-f} \\ (1 + \epsilon_{Nf}^m)k_{f-s} & -(1 + \epsilon_{Ns}^m)k_{s-f} \end{pmatrix} \end{cases}$$

(23b)

Table 3. Kinetic Rate Constants k_{f-s} and k_{s-f} Determined by Nonlinear Regression with Four-Parameter Fitting in Eq. 26a for the Case of $N = 1.0\times10^4$ and $t = 5.0\times10^{-5}$ s

K	V_f/V_s	k_{f-s} (s^{-1})	k_{s-f} (s^{-1})	k_{f-s}/k_{s-f}	Error (%)	$\tilde{N}_s/\tilde{N}_f$	Error (%)
500.0	2.0	16.86 ± 0.08	0.087 ± 0.007	194.54 ± 14.94	−22.19	254.02 ± 20.39	1.61
200.0	2.0	16.89 ± 0.09	0.19 ± 0.007	88.06 ± 3.28	−11.94	98.45 ± 7.81	−1.55
100.0	2.0	16.84 ± 0.09	0.37 ± 0.008	45.98 ± 1.03	−8.05	49.08 ± 1.53	−1.85
50.0	2.0	16.14 ± 0.08	0.66 ± 0.008	24.50 ± 0.32	−2.00	25.56 ± 0.60	2.23
20.0	2.0	14.89 ± 0.09	1.51 ± 0.01	9.87 ± 0.10	−1.35	10.04 ± 0.13	0.41
10.0	2.0	13.58 ± 0.08	2.73 ± 0.02	4.97 ± 0.05	−0.63	5.08 ± 0.06	1.55
5.0	2.0	11.16 ± 0.08	4.49 ± 0.04	2.49 ± 0.03	−0.47	2.53 ± 0.03	1.13
2.0	2.0	7.40 ± 0.05	7.38 ± 0.05	1.00 ± 0.009	0.26	1.00 ± 0.009	0.32
1.0	2.0	4.53 ± 0.03	9.05 ± 0.06	0.50 ± 0.005	0.21	0.50 ± 0.004	0.47
0.5	2.0	2.44 ± 0.02	9.71 ± 0.10	0.25 ± 0.004	0.62	0.25 ± 0.002	1.14
0.2	2.0	1.19 ± 0.02	11.98 ± 0.20	0.099 ± 0.002	−0.74	0.098 ± 0.002	−1.66
0.1	2.0	0.63 ± 0.009	12.73 ± 0.20	0.049 ± 0.001	−1.33	0.049 ± 0.001	−1.40
0.05	2.0	0.34 ± 0.007	13.47 ± 0.30	0.025 ± 0.0008	0.56	0.025 ± 0.0006	−1.00
0.02	2.0	0.14 ± 0.006	13.63 ± 0.62	0.010 ± 0.0006	0.53	0.010 ± 0.0006	−0.48
0.01	2.0	0.07 ± 0.004	15.25 ± 0.88	0.005 ± 0.0004	−6.21	0.005 ± 0.0003	−8.58

$$\text{(III)}\quad \begin{cases} \dfrac{dN_{\mathrm{III}}(T)}{dT} = A_{\mathrm{III}} N_{\mathrm{III}}(T) + f_{\mathrm{III}}(T) & \text{(24a)} \\ A_{\mathrm{III}} = A, \quad f_{\mathrm{III}}(T) = \begin{pmatrix} \epsilon_{Tf} \\ \epsilon_{Ts} \end{pmatrix} & \text{(24b)} \end{cases}$$

The leading and dominant terms in the solution of the ODE systems (I) to (III) are derived in the Appendix, and are given by

$$N_{\mathrm{I,\,II,\,III}}(T) = c_1 + c_2 \exp(-(k_{f-s} + k_{s-f})T) + c_3 T \exp(c_4 T) \tag{25}$$

where c_1, c_2, and c_3 are vectors, and c_4 is constant. In more detailed format

$$\begin{pmatrix} N_f \\ N_s \end{pmatrix} = \frac{N}{k_{f-s} + k_{s-f}} \times \begin{Bmatrix} k_{s-f} + k_{f-s} \exp[-(k_{f-s} + k_{s-f})T] + c_{3f} T \exp(c_{4f} T) \\ k_{f-s} - k_{f-s} \exp[-(k_{f-s} + k_{s-f})T] + c_{3s} T \exp(c_{4s} T) \end{Bmatrix} \tag{26a}$$

(26b)

For a given set of simulation data (T, N_f), the rate constants k_{f-s} and k_{s-f} together with the scalars c_{3f} and c_{4f} can be determined by applying nonlinear regression with a biexponential (four-parameter) fitting according to Eq. 26a. An example of this four-parameter fitting strategy is illustrated in Table 3, as well as in Figures 4 and 5.

Figures 4A and 4B provide a comparison of the rate constants obtained from the two-parameter and four-parameter regression equations. Both of these approaches describe the trend of the rate constants k_{f-s} and k_{s-f} with increasing distribution coefficient K, which is consistent with the theory in Eq. 5. The curve for k_{f-s} in Figure 4A increases rapidly, whereas that for k_{s-f} in Figure 4B decreases very slowly as $K(V_s/V_f)$ approaches unity, at which point k_{f-s} and k_{s-f} are equal. After this point, k_{s-f} decreases rapidly and k_{f-s} increases very slowly. In Figures 5A and 5B, the relative standard deviation for k_{f-s} and k_{s-f} is illustrated for the two-parameter and four-parameter regression equations. It is evident that the four-parameter approach shows better precision, especially for k_{s-f}. In addition, Figure 4C compares the ratio of the rate constants k_{f-s}/k_{s-f} obtained from the two-parameter and four-parameter regression equations. The ratio is closer to the theoretically expected value in Eq. 5 for the four-parameter approach, which is confirmed by comparing the relative error in Figure 5C. For the case where $K(V_s/V_f)$ is unity, the rate constants k_{f-s} and k_{s-f} are determined to be 7.40 ± 0.05 s^{-1} and 7.38 ± 0.05 s^{-1}, respectively. The ratio of these rate constants ($k_{f-s}/k_{s-f} = 1.00 \pm 0.009$) is in accord with the ratio of the number of molecules in the surface and fluid phases at equilibrium ($\tilde{N}_s/\tilde{N}_f = 1.00 \pm 0.009$). Similarly, the principle of detailed balance reveals that each molecule is transferred from fluid to surface phase

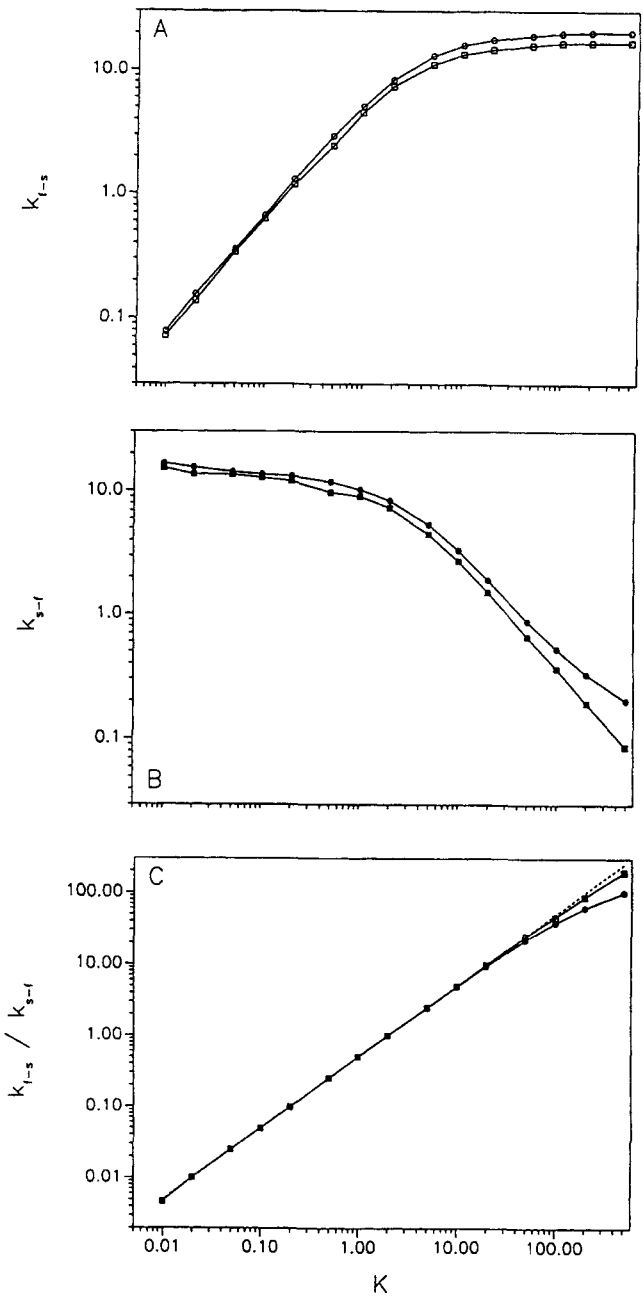

Figure 4. Individual rate constants k_{f-s} (A) and k_{s-f} (B), and the ratio of the rate constants k_{f-s}/k_{s-f} (C) determined by the two-parameter regression equation (○, ●, ⊕) and the four-parameter regression equation (□, ■, ⊞).

Simulation conditions: $N = 1.0 \times 10^4$; $t = 5.0 \times 10^{-5}$ s; $R = 20.0 \times 10^{-4}$ cm; $d_s = 4.49 \times 10^{-4}$ cm; $D_f = 1.0 \times 10^{-5}$ cm$^2 \cdot$ s^{-1}; $D_s = 1.0 \times 10^{-6}$ cm$^2 \cdot$ s^{-1}.

an average of 3.694 times per second, and from surface to fluid phase an average of 3.696 times per second at equilibrium, which are more commensurate than the values obtained with the two-parameter strategy (*vide supra*).

From these results, we may conclude that the four-parameter regression equation developed in this work, which pro-

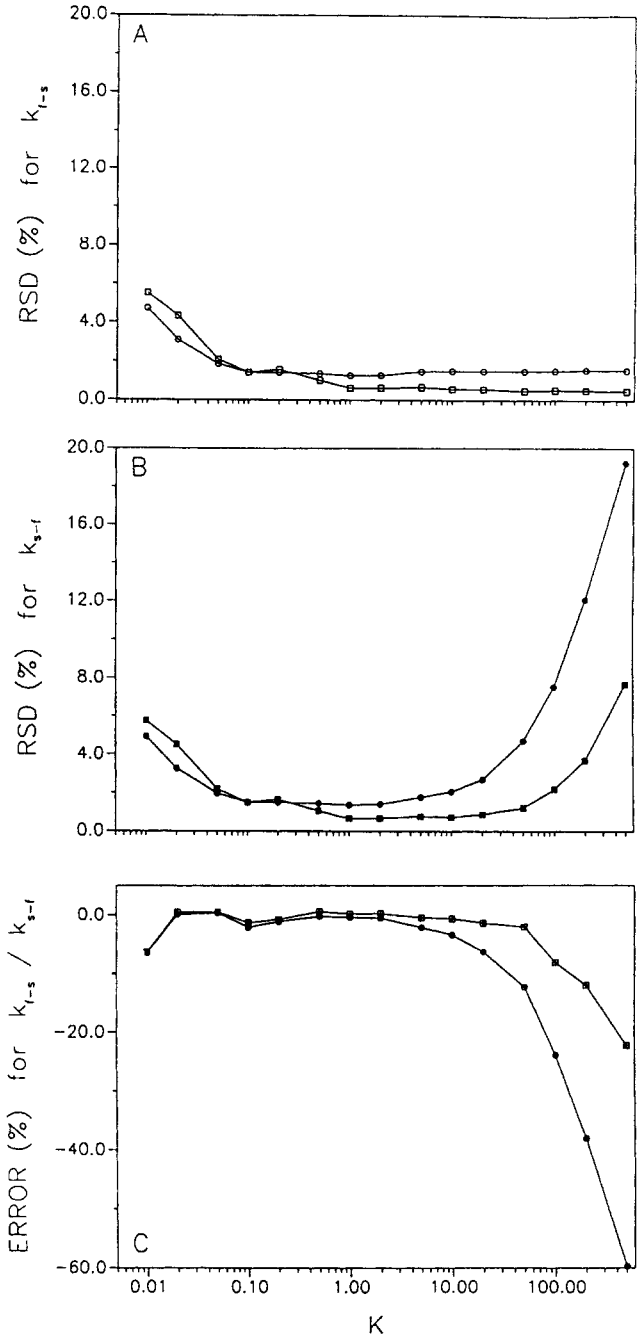

Figure 5. Relative standard deviation for the rate constants k_{f-s} (A) and k_{s-f} (B), and the error for the ratio of the rate constants k_{f-s}/k_{s-f} (C) determined by the two-parameter regression equation (○, ●, ⊕) and the four-parameter regression equation (□, ■, ⊞).

Simulation conditions: $N = 1.0\times10^{4}$; $t = 5.0\times10^{-5}$ s; $R = 20.0\times10^{-4}$ cm; $d_s = 4.49\times10^{-4}$ cm; $D_f = 1.0\times10^{-5}$ cm$^2\cdot$s^{-1}; $D_s = 1.0\times10^{-6}$ cm$^2\cdot$s^{-1}.

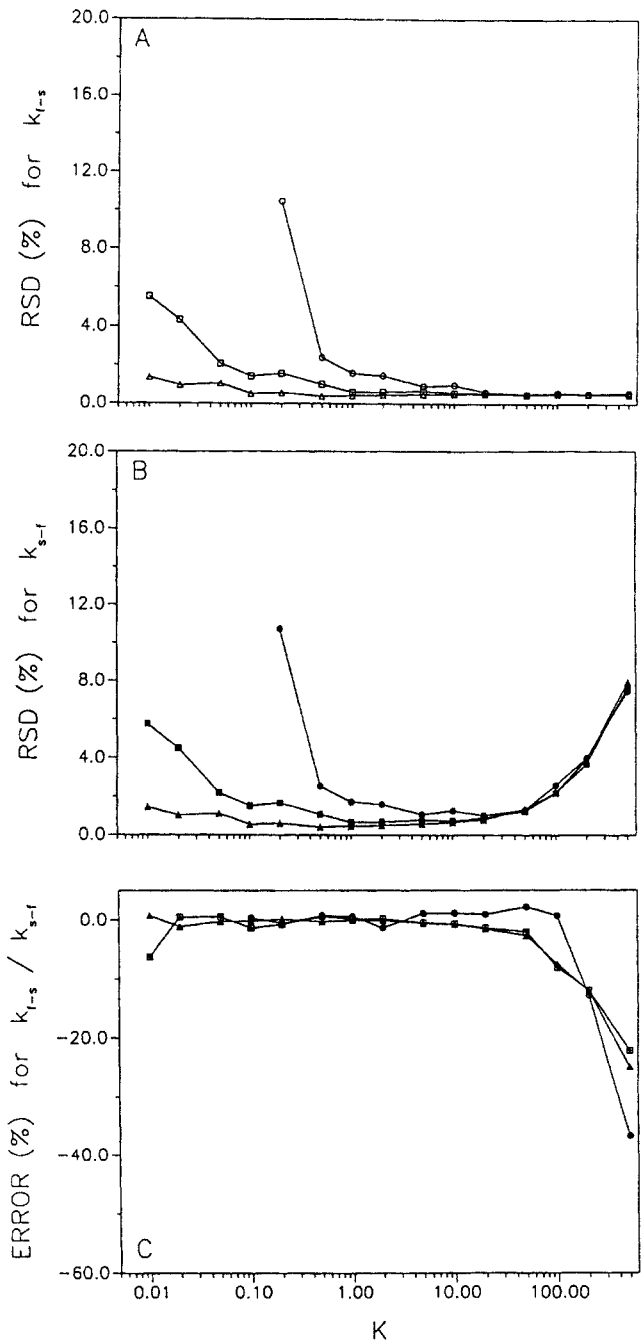

Figure 6. Relative standard deviation for the rate constants k_{f-s} (A) and k_{s-f} (B), and the error for the ratio of the rate constants k_{f-s}/k_{s-f} (C) as a function of the number of molecules.

Simulation conditions: $N = 1.0\times10^{3}$ (○, ●, ⊕), 1.0×10^{4} (□, ■, ⊞), 1.0×10^{5} (△, ▲,); $t = 5.0\times10^{-5}$ s; $R = 20.0\times10^{-4}$ cm; $d_s = 4.49\times10^{-4}$ cm; $D_f = 1.0\times10^{-5}$ cm$^2\cdot$s^{-1}; $D_s = 1.0\times10^{-6}$ cm$^2\cdot$s^{-1}.

vides correction for intrinsic numerical error, is superior to the classical two-parameter equation. Because this error arises from uncertainty in the number of molecules and time, we will examine next the effect of these variables on the accuracy and precision of rate constant determination.

Effect of number of molecules

The kinetic evolution of the absorption process has been examined over a wide range of distribution coefficients, as summarized in Tables 2 and 3. As the distribution coefficient K increases, the number of molecules in the fluid phase at equilibrium decreases as $\tilde{N}_f = N/[1+K(V_s/V_f)]$ and, con-

Table 4. Kinetic Rate Constants k_{f-s} and k_{s-f} Determined as Function of Simulation Data Range with Constant Density; Nonlinear Regression with Four-Parameter Fitting in Eq. 26a for the Case of $N = 1.0\times10^4$, $t = 1.0\times10^{-3}$ s, $K = 2.0$, and $V_f/V_s = 2.0$

Point Density	Point Range	k_{f-s} (s^{-1})	k_{s-f} (s^{-1})	k_{f-s}/k_{s-f}	Error (%)
60	1 τ	11.45±0.16	19.55±0.58	0.59±0.02	−41.44
60	2 τ	8.82±0.08	10.66±0.20	0.83±0.02	−17.22
60	3 τ	7.81±0.06	8.24±0.11	0.95±0.01	−5.27
60	4 τ	7.46±0.04	7.56±0.06	0.99±0.01	−1.33
60	5 τ	7.42±0.03	7.49±0.04	0.99±0.007	−0.89
60	7 τ	7.43±0.02	7.50±0.03	0.99±0.005	−0.99
60	10 τ	7.35±0.02	7.39±0.02	1.00±0.004	−0.44
60	15 τ	7.24±0.02	7.22±0.02	1.00±0.004	0.30
60	20 τ	7.18±0.02	7.13±0.02	1.01±0.004	0.72
60	30 τ	7.22±0.02	7.18±0.02	1.00±0.004	0.48
60	40 τ	7.23±0.02	7.20±0.02	1.00±0.003	0.41
60	50 τ	7.24±0.02	7.22±0.02	1.00±0.003	0.30
60	60 τ	7.27±0.02	7.26±0.02	1.00±0.003	0.12
60	70 τ	7.27±0.02	7.26±0.02	1.00±0.003	0.14
60	80 τ	7.28±0.02	7.27±0.02	1.00±0.003	0.07

versely, the number of molecules in the surface phase increases as $\tilde{N}_s = NK(V_s/V_f)/[1 + K(V_s/V_f)]$. For example, in the case where $K = 500.0$ and $N = 1{,}000$, there are approximately four molecules in the fluid phase and 996 molecules in the surface phase at equilibrium. If the statistical variation of the stochastic simulation is ±1 molecule, then the small number of molecules in the fluid phase limits the precision and accuracy of $\tilde{N}_f$ to ±25%, ±2 molecules limits $\tilde{N}_f$ to ±50%, and so on. This quantified source of error may be reduced by increasing the total number of molecules in the simulation. For example, in the case cited above, ±1 molecule limits $\tilde{N}_f$ to ±25% for $N = 1.0\times10^3$, ±2.5% for $N = 1.0\times10^4$, and ±0.25% for $N = 1.0\times10^5$. A similar problem arises for distribution coefficients significantly less than unity, where the number of molecules in the surface phase becomes the limiting factor.

Although the four-parameter regression strategy provides compensation for certain sources of numerical error that are related to the number of molecules, such compensation may not be ideal or exhaustive. It is, therefore, necessary to examine the precision and accuracy of the rate constants k_{f-s} and k_{s-f} as well as their ratio k_{f-s}/k_{s-f} as a function of the total number of molecules. As shown in Figures 6A and 6B, the relative standard deviation of the rate constants improves significantly with the number of molecules for distribution coefficients less than unity, but only slightly for those greater than unity. The ratio of the rate constants in Figure 6C shows error that is small and relatively independent of the number of molecules for distribution coefficients from 0.01 to 100.0. Above this point, the error increases and is most significant for the smaller number of molecules. Thus, it is necessary for the total number of molecules to be sufficiently large to overcome the quantified error discussed above in order to achieve the desired level of statistical accuracy and precision.

Effect of time increment and range

The accuracy and precision also depend on the time domain of the simulation data that are used in the regression analysis. For convenience in normalization of the simulation data, we will define the density in terms of the number of data points in the characteristic time τ, and the range in terms of the number of multiples of the time τ. The effect of the time range with constant density is summarized in Table 4. When the range is less than 5τ, the simulation has not yet reached steady-state conditions and the rate constants are systematically overestimated. Because all molecules initially reside in the fluid phase, the rate constant k_{s-f} is overestimated to a greater extent than k_{f-s}, which results in significant negative error in the ratio k_{f-s}/k_{s-f}. When the range exceeds 10τ, the rate constants approach a limiting value and their ratio accurately reflects the equilibrium constant according to Eq. 5. The precision of the rate constants, expressed as the reciprocal of the relative standard deviation, is illustrated as a function of the time range in Figure 7. For

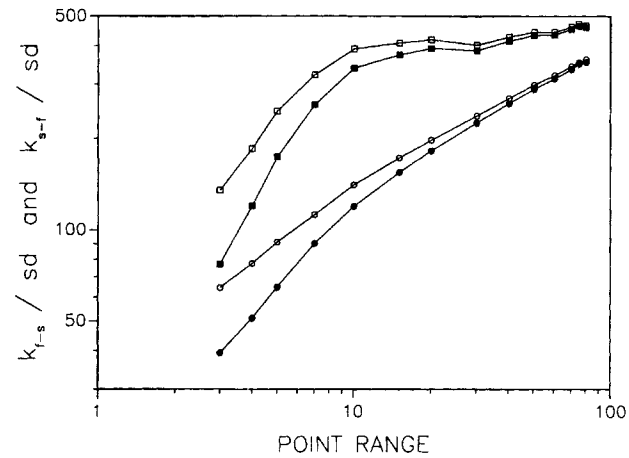

Figure 7. Reciprocal of the relative standard deviation for the rate constants k_{f-s} and k_{s-f} determined by the two-parameter regression equation (○, ●) and the four-parameter regression equation (□, ■) as a function of the simulation data range with constant density.

Simulation conditions: $N = 1.0\times10^4$; $t = 1.0\times10^{-3}$ s; $R = 20.0\times10^{-4}$ cm; $d_s = 4.49\times10^{-4}$ cm; $D_f = 1.0\times10^{-5}$ cm$^2\cdot$s^{-1}; $D_s = 1.0\times10^{-6}$ cm$^2\cdot$s^{-1}; $K = 2.0$.

the two-parameter regression strategy, the precision for k_{s-f} increases linearly with the range up to 10τ and with the square root of the range thereafter, whereas the precision for k_{f-s} increases with the square root of the range up to 10τ and slightly less thereafter. In contrast, the four-parameter regression strategy provides some compensation for numerical error that is related to time and, hence, shows distinctly different behavior. The precision for k_{s-f} increases with the 3/2 power of the range up to 10τ, whereas the precision for k_{f-s} increases linearly with the range up to 10τ. The precision for both rate constants becomes independent of the range after approximately 15 to 20τ, which suggests that this range may be considered optimal for the statistical regression analysis.

The effect of the time density with constant range is summarized in Table 5. Although a small error arises when the density is less than 10 points in τ, the accuracy of the rate constants is relatively unaffected by time density from 10 to 600 points in τ. The precision of the rate constants, expressed as the reciprocal of the relative standard deviation, is illustrated as a function of the density in Figure 8. The precision for both k_{f-s} and k_{s-f} improves consistently with the square root of the density for both the two-parameter and four-parameter regression strategies. Because there is no change in the rate of improvement, the optimal density may be determined from Figure 8 for any desired level of precision. For example, 0.5% RSD would require approximately 100 points in τ for the two-parameter strategy but only 20 points in τ for the four-parameter strategy.

Finally, we consider the effect of the time increment of the simulation. The molecular diffusion distance in Eq. 1 increases with the square root of the time increment, whereas the total number of diffusion steps in a given simulation time is inversely related to the time increment. Therefore, the total distance traveled in a given simulation time varies inversely with the square root of the time increment. It seems reasonable to surmise that a small time increment, which provides a greater number of small diffusion steps in the fluid and surface phases, may provide a more accurate simulation of the absorption process. The effect of the time increment, maintaining a constant density and range of data for the re-

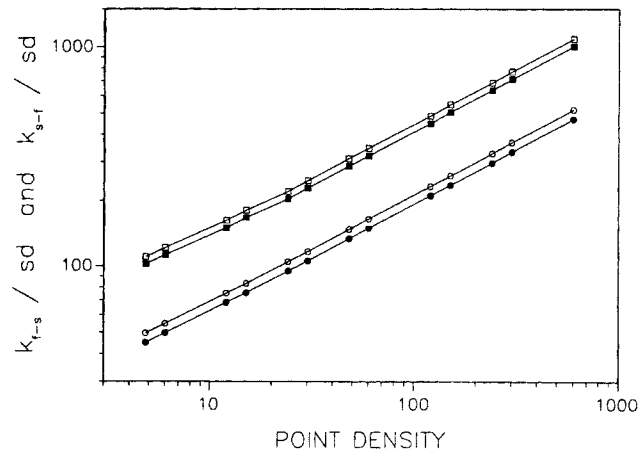

Figure 8. Reciprocal of the relative standard deviation for the rate constants k_{f-s} and k_{s-f} determined by the two-parameter regression equation (○, ●) and the four-parameter regression equation (□, ■) as a function of the simulation data density with constant range.

Simulation conditions: $N = 1.0\times10^{4}$; $t = 5.0\times10^{-5}$ s; $R = 20.0\times10^{-4}$ cm; $d_s = 4.49\times10^{-4}$ cm; $D_f = 1.0\times10^{-5}$ cm$^2\cdot$s^{-1}; $D_s = 1.0\times10^{-6}$ cm$^2\cdot$s^{-1}; $K = 2.0$.

Table 5. Kinetic Rate Constants k_{f-s} and k_{s-f} Determined as Function of Simulation Data Density with Constant Range; Nonlinear Regression with Four-Parameter Fitting in Eq. 26a for the Case of $N = 1.0\times10^{4}$, $K = 2.0$, and $V_f/V_s = 2.0$

Point Density	Point Range	k_{f-s} (s^{-1})	k_{s-f} (s^{-1})	k_{f-s}/k_{s-f}	Error (%)
5	15 τ	7.04 ± 0.06	7.04 ± 0.07	1.00 ± 0.01	0.05
6	15 τ	7.10 ± 0.06	7.10 ± 0.06	1.00 ± 0.01	−0.003
12	15 τ	7.16 ± 0.04	7.17 ± 0.05	1.00 ± 0.009	−0.07
15	15 τ	7.13 ± 0.04	7.13 ± 0.04	1.00 ± 0.008	0.01
24	15 τ	7.15 ± 0.03	7.15 ± 0.04	1.00 ± 0.007	−0.05
30	15 τ	7.15 ± 0.03	7.15 ± 0.03	1.00 ± 0.006	−0.03
48	15 τ	7.15 ± 0.02	7.16 ± 0.02	1.00 ± 0.005	−0.02
60	15 τ	7.15 ± 0.02	7.15 ± 0.02	1.00 ± 0.004	−0.05
120	15 τ	7.15 ± 0.01	7.15 ± 0.02	1.00 ± 0.003	−0.03
150	15 τ	7.15 ± 0.01	7.15 ± 0.01	1.00 ± 0.003	−0.04
240	15 τ	7.15 ± 0.01	7.15 ± 0.01	1.00 ± 0.002	−0.03
300	15 τ	7.15 ± 0.009	7.15 ± 0.01	1.00 ± 0.002	−0.04
600	15 τ	7.15 ± 0.007	7.15 ± 0.007	1.00 ± 0.001	−0.03

Table 6. Kinetic Rate Constants k_{f-s} and k_{s-f} Determined as Function of Simulation Time Constant (t) with Constant Density and Range; Nonlinear Regression with Four-Parameter Fitting in Eq. 26a for the Case of $N = 1.0\times10^{4}$, $K = 2.0$, and $V_f/V_s = 2.0$

t (s)	Point Density	Point Range	k_{f-s} (s^{-1})	k_{s-f} (s^{-1})	k_{f-s}/k_{s-f}	Error (%)
5.0×10^{-6}	12	15 τ	7.38 ± 0.05	7.35 ± 0.05	1.00 ± 0.01	0.41
5.0×10^{-5}	12	15 τ	7.40 ± 0.05	7.38 ± 0.05	1.00 ± 0.009	0.26
5.0×10^{-4}	12	15 τ	7.74 ± 0.04	7.88 ± 0.04	0.98 ± 0.007	−1.87
5.0×10^{-3}	12	15 τ	7.12 ± 0.04	7.18 ± 0.04	0.99 ± 0.007	−0.78

gression analysis, is summarized in Table 6. The accuracy and precision of the rate constants k_{f-s} and k_{s-f}, as well as their ratio k_{f-s}/k_{s-f}, remain relatively constant with time increments from 5.0×10^{-3} s to 5.0×10^{-6} s. Thus, it does not appear to be beneficial to reduce the time increment below that necessary for good statistical representation of the data.

Effect of initial conditions

In all of the studies described thus far, we have employed the initial condition (i) where all molecules reside in the fluid phase. As the system begins the kinetic evolution toward the steady state, shown in Figure 2, there are initially no molecules that undergo the transition from surface to fluid phase. Consequently, k_{s-f} cannot be estimated as reliably as k_{f-s} from the nonlinear regression strategy. This source of error is particularly problematic for high distribution coefficients, where k_{s-f} is intrinsically small, as evident in the comparison of Figures 6A and 6B. Moreover, this source of error cannot be corrected by means of the number of molecules or the time increment. As shown in Figure 6B, an increase in the number of molecules has little or no effect on the precision of k_{s-f} for distribution coefficients greater than 20.0. Because the precision of k_{f-s} is significantly better under comparable conditions (that is, distribution coefficients less than 0.2), it seems desirable to examine the effect of the initial conditions on the accuracy and precision of the rate constants.

Consider the case wherein all molecules reside initially in the surface phase, and the number of molecules remaining in the surface phase is monitored as a function of time. The solution to the ODE system in Eq. 9 associated with the initial condition (ii) is given by Eq. 17b. For a given set of simulation data (T, N_s), the rate constants k_{f-s} and k_{s-f} can be determined by applying nonlinear regression with an exponential (two-parameter) fitting according to Eq. 17b.

Alternatively, an error analysis may be applied to the ODE system associated with the initial condition (ii), as shown in the Appendix. The leading and dominant terms of the solution are given in detailed format as

$$\begin{pmatrix} N_f \\ N_s \end{pmatrix} = \frac{N}{k_{f-s}+k_{s-f}} \times \begin{Bmatrix} k_{s-f} - k_{s-f}\exp[-(k_{f-s}+k_{s-f})T] + c_{3f}T\exp(c_{4f}T) \\ k_{f-s} + k_{s-f}\exp[-(k_{f-s}+k_{s-f})T] + c_{3s}T\exp(c_{4s}T) \end{Bmatrix} \quad \text{(27a)}$$

(27b)

This solution is directly analogous to Eqs. 26a and 26b for the ODE systems (I) to (III) associated with the initial condition (i). For the set of simulation data (T, N_s), the rate constants k_{f-s} and k_{s-f} together with the scalars c_{3s} and c_{4s} can be determined by applying nonlinear regression with a biexponential (four-parameter) fitting according to Eq. 27b. An example of this four-parameter fitting strategy is illustrated in Table 7, as well as in Figures 9 and 10.

Figures 9A and 9B provide a comparison of the rate constants obtained with initial conditions (i) and (ii), hereafter called the N_f-strategy and N_s-strategy, respectively. It is apparent that the values for both k_{f-s} and k_{s-f} are systematically lower by using the N_s-strategy, which is verified by comparison of Tables 3 and 7. The relative standard deviation, illustrated in Figures 10A and 10B, suggests that the precision for k_{f-s} is best using the N_s-strategy at low distribution coefficients and the N_f-strategy at high distribution coefficients, whereas the precision for k_{s-f} is uniformly better using the N_s-strategy. In addition, the ratio of the rate constants k_{f-s}/k_{s-f} is shown in Figure 9C with the corresponding errors in Figure 10C. From these results, we may conclude that the N_f- and N_s-strategies are complementary and show superior performance for distribution coefficients that are lower and higher than unity, respectively.

Conclusions

In this study, a numerical approach has been developed to determine the individual rate constants and the ratio of the rate constants from stochastic computer simulations. A biexponential (four-parameter) equation, which provides for in-

Table 7. Kinetic Rate Constants k_{f-s} and k_{s-f} Determined by Nonlinear Regression with Four-Parameter Fitting in Eq. 27b for the Case of $N = 1.0\times10^4$ and $t = 5.0\times10^{-5}$ s

K	V_f/V_s	k_{f-s} (s^{-1})	k_{s-f} (s^{-1})	k_{f-s}/k_{s-f}	Error (%)	$\tilde{N}_s/\tilde{N}_f$	Error (%)
500.0	2.0	13.27±0.97	0.053±0.004	252.40±25.28	0.96	250.93±41.18	0.37
200.0	2.0	16.94±0.48	0.17±0.005	100.47±3.94	0.47	101.93±4.06	1.93
100.0	2.0	14.38±0.27	0.29±0.005	49.76±1.28	−0.49	49.87±1.29	−0.27
50.0	2.0	15.30±0.25	0.61±0.009	24.98±0.56	−0.07	25.22±0.72	0.88
20.0	2.0	13.29±0.12	1.32±0.01	10.10±0.12	0.96	10.16±0.18	1.55
10.0	2.0	11.99±0.09	2.38±0.02	5.03±0.05	0.60	5.06±0.07	1.19
5.0	2.0	9.75±0.06	3.87±0.02	2.52±0.02	0.64	2.54±0.02	1.44
2.0	2.0	6.26±0.02	6.27±0.02	1.00±0.004	−0.19	0.99±0.006	−0.97
1.0	2.0	3.96±0.01	7.94±0.02	0.50±0.002	−0.24	0.50±0.002	−0.06
0.5	2.0	2.27±0.005	9.11±0.01	0.25±0.0007	−0.49	0.25±0.002	−0.07
0.2	2.0	1.03±0.003	10.26±0.02	0.10±0.0003	0.02	0.10±0.001	1.07
0.1	2.0	0.56±0.007	11.34±0.12	0.050±0.0008	−0.48	0.050±0.001	0.87
0.05	2.0	0.28±0.001	10.69±0.007	0.026±0.0001	3.23	0.026±0.001	2.28
0.02	2.0	0.11±0.0009	10.79±0.009	0.010±0.00009	−0.22	0.010±0.0006	4.87
0.01	2.0	0.05±0.0008	10.76±0.008	0.0046±0.00007	−7.23	0.005±0.0003	2.41

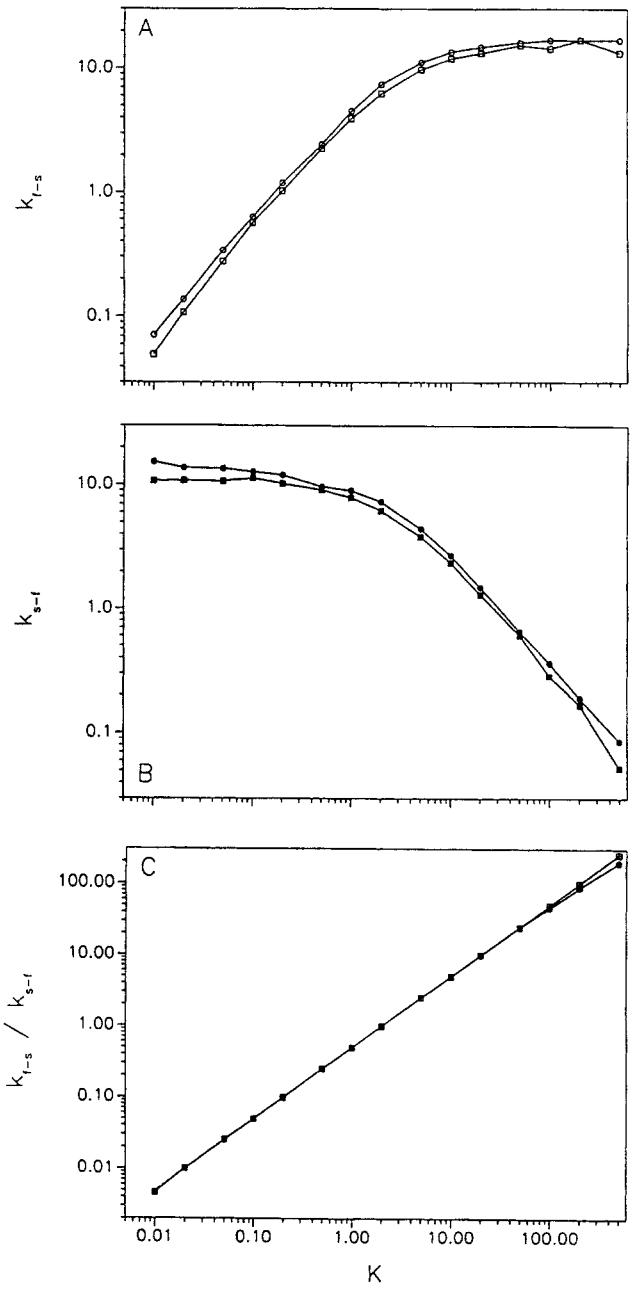

Figure 9. Individual rate constants k_{f-s} (A) and k_{s-f} (B), and the ratio of the rate constants k_{f-s}/k_{s-f} (C) determined by using the N_f-strategy (○, ●, ⊕) and the N_s-strategy (□, ■, ⊞).

Simulation conditions: $N = 1.0\times10^{4}$; $t = 5.0\times10^{-5}$ s; $R = 20.0\times10^{-4}$ cm; $d_s = 4.49\times10^{-4}$ cm; $D_f = 1.0\times10^{-5}$ cm$^2\cdot$s^{-1}; $D_s = 1.0\times10^{-6}$ cm$^2\cdot$s^{-1}.

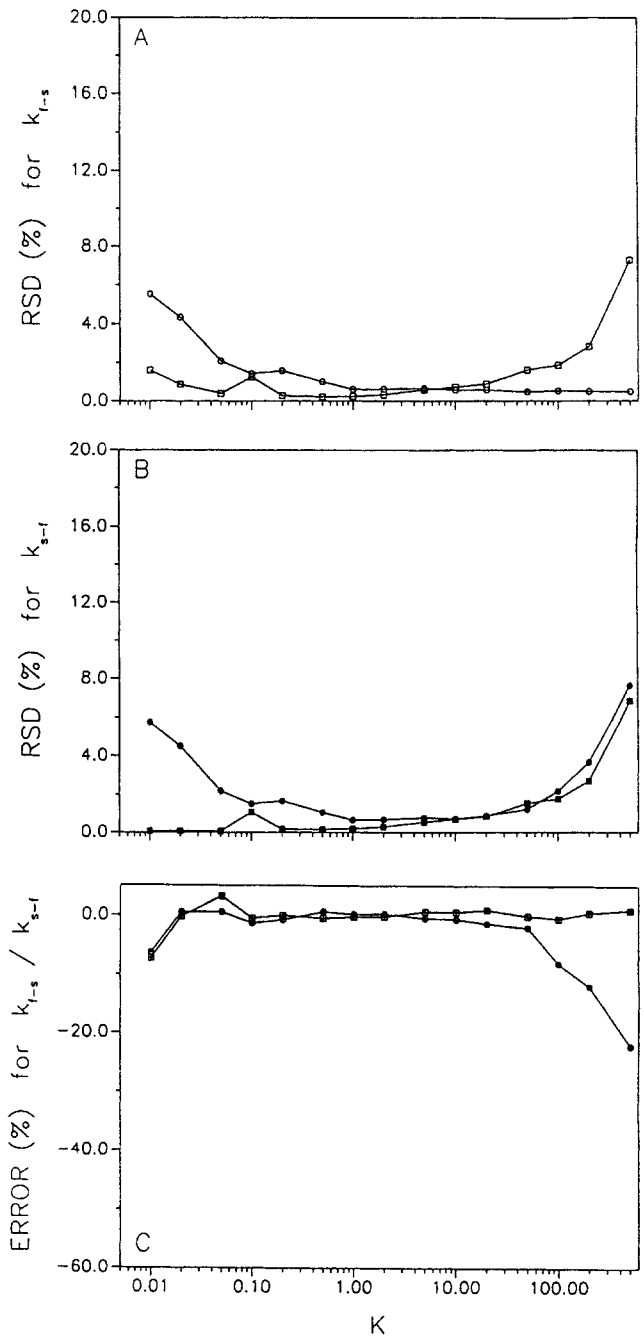

Figure 10. Relative standard deviation for the rate constants k_{f-s} (A) and k_{s-f} (B), and the error for the ratio of the rate constants k_{f-s}/k_{s-f} (C) determined by using the N_f-strategy (○, ●, ⊕) and the N_s-strategy (□, ■, ⊞).

Simulation conditions: $N = 1.0\times10^{4}$; $t = 5.0\times10^{-5}$ s; $R = 20.0\times10^{-4}$ cm; $d_s = 4.49\times10^{-4}$ cm; $D_f = 1.0\times10^{-5}$ cm$^2\cdot$s^{-1}; $D_s = 1.0\times10^{-6}$ cm$^2\cdot$s^{-1}.

herent correction of numerical error, is shown to be superior to the classical exponential (two-parameter) regression equation. The effects of the initial conditions, the number of molecules, and the time domain are examined in detail to ascertain the most favorable simulation conditions. This approach has been demonstrated for an absorption system with homogeneous fluid and surface phases under diffusion-limited conditions. Because the kinetic and steady-state behavior of this simple first-order system are well known as a function of the simulation variables, it is possible to evaluate the statistical accuracy and precision of the regression approach. This approach has been successfully applied for distribution coefficients ranging from 0.01 to 100.0, yielding individual rate constants k_{f-s} and k_{s-f} with $\pm0.84\%$ and

$\pm 0.57\%$ average relative standard deviation, and the ratio of the rate constants with $\pm 1.04\%$ average relative standard deviation and $\pm 1.14\%$ average relative error. On the basis of these validation studies, this approach may now be applied with confidence to evaluate more complicated systems such as fluids or surfaces that exhibit heterogeneity at the molecular, microscopic, or macroscopic level. Furthermore, it may be extended to more elaborate mass-transport and chemical processes such as second- and higher-order kinetics as well as mixed mechanisms from absorption/adsorption, absorption/reaction, and adsorption/reaction, in the absence or presence of convective flow. Hence, this approach provides the opportunity to characterize and to gain much-needed insight to the kinetic and steady-state behavior of complex systems.

Acknowledgments

This research was sponsored by the U.S. Dept. of Energy, Office of Basic Energy Sciences, Division of Chemical Sciences, under contract number DE-FG02-89ER14056. In addition, partial financial support for the IBM RS/6000 Model 580 computer was received from Michigan State University Computing and Technology Dept. P.W. gratefully acknowledges support by the Center for Fundamental Materials Research, College of Natural Science, and Depts. of Chemistry and Mathematics, as well as the Office of the Provost for an Affirmative Action Postdoctoral Fellowship.

Literature Cited

Barzykin, A. V., and M. Tachiya, "Diffusive Transport Across an Interface," *J. Phys. Chem. B*, **102**, 3192 (1998).

Benson, S. W., *Foundations of Chemical Kinetics*, McGraw-Hill, New York (1960).

Betteridge, D., C. Z. Marczewski, and A. P. Wade, "A Random Walk Simulation of Flow Injection Analysis," *Anal. Chim. Acta*, **165**, 227 (1984).

Binder, K., *Monte Carlo Method in Statistical Physics, Topics in Current Physics*, 2nd ed., Vol. 7, Springer-Verlag, Berlin (1986).

Binder, K., *Applications of the Monte Carlo Methods in Statistical Physics, Topics in Current Physics*, 2nd ed., Vol. 36, Springer-Verlag, Berlin (1987).

Bowker, M., and D. A. King, "Adsorbate Diffusion on Single-Crystal Surfaces. I. Influence of Lateral Interactions," *Surf. Sci.*, **71**, 583 (1978a).

Bowker, M., and D. A. King, "Adsorbate Diffusion on Single-Crystal Surfaces. II. Extension to Next Nearest Neighbor Interactions," *Surf. Sci.*, **72**, 208 (1978b).

Burganos, V. N., and S. V. Sotirchos, "Simulation of Knudsen Diffusion in Random Networks of Parallel Pores," *Chem. Eng. Sci.*, **43**, 1685 (1988).

Burganos, V. N., and S. V. Sotirchos, "Knudsen Diffusion in Parallel, Multidimensional, or Randomly Oriented Capillary Structures," *Chem. Eng. Sci.*, **44**, 2451 (1989).

Celenligil, M. C., G. A. Bird, and J. N. Moss, "Direct Simulation of Three-Dimensional Hypersonic Flow About Intersecting Blunt Wedges," *AIAA J.*, **27**, 1536 (1989).

Einstein, A., "Motion of Suspended Particles in the Kinetic Theory," *Ann. Phys.*, **17**, 549 (1905).

Feller, W., *Probability Theory and its Application*, Chapter 14, Wiley, New York (1950).

Fichthorn, K. A., and W. H. Weinberg, "Theoretical Foundations of Dynamical Monte Carlo Simulations," *J. Chem. Phys.*, **95**, 1090 (1991).

Gupta, D., and C. S. Hirtzel, "Monte Carlo Simulation of Temperature-Programmed Desorption of Molecules from Solid Surfaces," *Chem. Phys. Lett.*, **149**, 527 (1984).

Hood, E. S., B. H. Toby, and W. H. Weinberg, "Precursor-Mediated Molecular Chemisorption and Thermal Desorption: The Interrelationships among Energetics, Kinetics, and Adsorbate Lattice Structure," *Chem. Phys. Lett.*, **55**, 2437 (1985).

Hopkins, D. L., and V. L. McGuffin, "Three-Dimensional Molecular Simulation of Electrophoretic Separations," *Anal. Chem.*, **70**, 1066 (1998).

Kang, H. C., T. A. Jachimowski, and W. H. Weinberg, "Role of Local Configurations in a Langmuir–Hinshelwood Surface Reaction: Kinetics and Compensation," *J. Chem. Phys.*, **93**, 1418 (1990).

Kang, H. C., and W. H. Weinberg, "Dynamic Monte Carlo with a Proper Energy Barrier: Surface Diffusion and Two-Dimensional Domain Ordering," *J. Chem. Phys.*, **90**, 2824 (1989).

Kang, H. C., and W. H. Weinberg, "Dynamic Monte Carlo Simulations of Surface-Rate Processes," *Acc. Chem. Res.*, **25**, 253 (1992).

Kawasaki, K., "Diffusion Constants Near the Critical Point for Time-Dependent Ising Models. Part I," *Phys. Rev.*, **145**, 224 (1966a).

Kawasaki, K., "Diffusion Constants Near the Critical Point for Time-Dependent Ising Models. Part II," *Phys. Rev.*, **148**, 375 (1966b).

Kawasaki, K., "Diffusion Constants Near the Critical Point for Time-Dependent Ising Models. Part III," *Phys. Rev.*, **150**, 285 (1966c).

Kutner, R., K. Binder, and K. W. Kehr, "Diffusion in Concentrated Lattice Gases. II. Particles with Attractive Nearest-Neighbor Interaction on Three-Dimensional Lattices," *Phys. Rev. B.*, **26**, 2967 (1982).

Kutner, R., K. Binder, and K. W. Kehr, "Diffusion in Concentrated Lattice Gases. V. Particles with Repulsive Nearest-Neighbor Interaction on the Face-Centered-Cubic Lattices," *Phys. Rev. B*, **28**, 1846 (1983).

Mak, C. H., H. C. Andersen, and S. M. George, "Monte Carlo Studies of Diffusion on Inhomogeneous Surfaces," *J. Chem. Phys.*, **88**, 4052 (1988).

McGuffin, V. L., P. Wu, and D. L. Hopkins, "Three-Dimensional Computer Simulation of Chromatographic and Electrophoretic Separations," *Proc. of Int. Symp. on Chromatography*, H. Hatano and T. Hanai, eds., World Scientific Publishing, River Edge, NJ, pp. 45–69 (1995).

McGuffin, V. L., and P. Wu, "Three-Dimensional Molecular Simulation of Chromatographic Separations," *J. Chromatogr.*, **722**, 3 (1996).

Morita, A., "Nonequilibrium Partition Constants," *J. Phys. Chem.*, **100**, 12131 (1996).

Murch, G. E., "Chemical Diffusion in Highly Defective Solids," *Philos. Mag. A*, **41**, 157 (1980).

Patrykiejew, A., "Phase Transitions in Adsorbed Layers. II. A Simple Theory Exhibiting Two Phase Transitions in Monolayer Films of Gases on Homogeneous Solid Surfaces," *Thin Solid Films*, **81**, 89 (1981).

Patrykiejew, A., "Phase Transitions in Adsorbed Layers. III. The Influence of Structural Factors on the Properties of Monolayers," *Thin Solid Films*, **88**, 359 (1982).

Patrykiejew, A., "Phase Transitions in Adsorbed Layers. IV. Thermodynamics of Monolayer Adsorption," *Thin Solid Films*, **105**, 259 (1983).

Patrykiejew, A., "Phase Transitions in Adsorbed Layers. VII. A Model for Mixed Gas Adsorption on Solid Surfaces," *Thin Solid Films*, **147**, 333 (1987).

Patrykiejew, A., "Phase Transitions in Adsorbed Layers. IX. The Influence of Geometric and Energetic Factors on Gas–Liquid–Solid Equilibria in Two-Component Monolayers Formed on Crystalline Solid Surfaces," *Thin Solid Films*, **161**, 351 (1988).

Patrykiejew, A., "Monte Carlo Studies of Adsorption. III. Localized Monolayers on Randomly Heterogeneous Surfaces," *Thin Solid Films*, **208**, 189 (1992).

Patrykiejew, A., and M. Jaroniec, "Partially Mobile Adsorption of Gases on Solid Surfaces," *Adv. Colloid Interface Sci.*, **20**, 273 (1984).

Ray, L. A., and R. C. Baetzold, "A Monte Carlo Estimation of Surface Diffusion by Simulating Laser-Induced Thermal Desorption," *J. Chem. Phys.*, **93**, 287 (1990).

Reid, R. C., J. M. Prausnitz, and T. K. Sherwood, *The Properties of Gases and Liquids*, McGraw-Hill, New York (1977).

Sadiq, A., and K. Binder, "Diffusion of Adsorbed Atoms in Ordered and Disordered Monolayers at Surfaces," *Surf. Sci.*, **128**, 350 (1983).

Schure, M. R., "Digital Simulation of Sedimentation Field-Flow Fractionation," *Anal. Chem.*, **60**, 1109 (1988).

Schure, M. R., and S. K. Weeratunga, "Coriolis-Induced Secondary Flow in Sedimentation Field-Flow Fractionation," *Anal. Chem.*, **63**, 2614 (1991).

Schure, M. R., and A. M. Lenhoff, "Consequences of Wall Adsorption in Capillary Electrophoresis: Theory and Simulation," *Anal. Chem.*, **65**, 3024 (1993).
Silverberg, M., and. A. Ben-Shaul, "Adsorbate Islanding in Surface Reactions: A Combined Monte Carlo–Lattice Gas Approach," *J. Chem. Phys.*, **87**, 3178 (1987).
Silverberg, M., A. Ben-Shaul, and F. Rebentrost, "On the Effects of Adsorbate Aggregation on the Kinetics of Surface Reactions," *J. Chem. Phys.*, **83**, 6501 (1985).
Sotirchos, S. V., "Multicomponent Diffusion and Convection in Capillary Structures," *AIChE J.*, **35**, 1953 (1989).
Steinfeld, J. I., J. S. Francisco, and W. L. Hase, *Chemical Kinetics and Dynamics*, Prentice Hall, Englewood Cliffs, NJ (1989).
Stiles, M., and H. Metiu, "On the Interplay Between Chemical Reactions and Phase Transitions for Molecules Adsorbed on Solid Surfaces," *Chem. Phys. Lett.*, **128**, 337 (1986).
Tomadakis, M. M., and S. V. Sotirchos, "Effective Knudsen Diffusivities in Structures of Randomly Overlapping Fibers," *AIChE J.*, **37**, 74 (1991a).
Tomadakis, M. M., and S. V. Sotirchos, "Knudsen Diffusivities and Properties of Structures of Unidirectional Fibers," *AIChE J.*, **37**, 1175 (1991b).
Tomadakis, M. M., and S. V. Sotirchos, "Ordinary and Transition Regime Diffusion in Random Fiber Structures," *AIChE J.*, **39**, 397 (1993a).
Tomadakis, M. M., and S. V. Sotirchos, "Ordinary, Transition, and Knudsen Regime Diffusion in Random Capillary Structures," *Chem. Eng. Sci.*, **48**, 3323 (1993b).
Wentzell, P. D., M. R. Bowridge, E. L. Taylor, and C. MacDonald, "Random Walk Simulation of Flow Injection Analysis: Evaluation of Dispersion Profiles," *Anal. Chim. Acta*, **278**, 293 (1993).

Appendix

By standard theory, the solution of the ODE system (I) is given by

$$N_I(T) = c_1 \exp(\lambda_1 T) + c_2 \exp(\lambda_2 T) \tag{A1}$$

where

$$\lambda_1 = 0 \quad \text{and} \quad \lambda_2 = -(k_{f-s} + k_{s-f} + \epsilon^a_{Nf} + \epsilon^a_{Ns}) \tag{A2}$$

are the eigenvalues of the matrix A_1 in Eq. 22b. By the Taylor expansion

$$\begin{aligned}\exp(\lambda_2 T) &= \exp[-(k_{f-s} + k_{s-f} + \epsilon^a_{Nf} + \epsilon^a_{Ns})T] \\ &= \exp(-(k_{f-s} + k_{s-f})T) - (\epsilon^a_{Nf} + \epsilon^a_{Ns})T \\ &\quad \times \exp[-(k_{f-s} + k_{s-f})T] + o(\epsilon^a_{Nf} + \epsilon^a_{Ns})\end{aligned}$$

where $o(\epsilon^a_{Nf} + \epsilon^a_{Ns})$ represents the truncated terms that tend to zero much faster than the errors ϵ^a_{Nf} and ϵ^a_{Ns}. Thus, by substitution into Eq. A1, we obtain the leading and dominant terms of $N_I(T)$

$$c_1 + c_2 \exp[-(k_{f-s} + k_{s-f})T] + c_3 T \exp(c_4 T) \tag{A3}$$

where c_1, c_2, and c_3 are vectors, and c_4 is constant. Similarly, we have the following equation for the ODE system (II)

$$N_{II}(T) = c_1 \exp(\lambda_1 T) + c_2 \exp(\lambda_2 T) \tag{A4}$$

where

$$\lambda_1 = 0 \quad \text{and} \quad \lambda_2 = -(k_{f-s} + k_{s-f} + \epsilon^m_{Nf} k_{f-s} + \epsilon^m_{Ns} k_{s-f}) \tag{A5}$$

and, hence,

$$\begin{aligned}\exp(\lambda_2 T) &= \exp[-(k_{f-s} + k_{s-f} + \epsilon^m_{Nf} k_{f-s} + \epsilon^m_{Ns} k_{s-f})T] \\ &= \exp[-(k_{f-s} + k_{s-f})T] - (\epsilon^m_{Nf} k_{f-s} + \epsilon^m_{Ns} k_{s-f})T \\ &\quad \times \exp[-(k_{f-s} + k_{s-f})T] + o(\epsilon^m_{Nf} + \epsilon^m_{Ns})\end{aligned}$$

Therefore, the leading and dominant terms of $N_{II}(T)$ are

$$c_1 + c_2 \exp[-(k_{f-s} + k_{s-f})T] + c_3 T \exp(c_4 T) \tag{A6}$$

where c_1, c_2, and c_3 are vectors, and c_4 is constant. Lastly, let us solve the ODE system (III). By multiplying $\exp(-TA)$ on both sides of Eq. 24a, we obtain

$$\frac{d}{dT}[\exp(-TA) N_{III}(T)] = \exp(-TA) f_{III}(T)$$

Integration of both sides of this equation leads to

$$N_{III}(T) = \exp(TA) N_0 + \exp(TA) \int_0^T \exp(-sA) f_{III}(s) ds \tag{A7}$$

We may reasonably infer that the error $f_{III}(T)$ in Eq. 24a was introduced when approximating Eq. 9 by using the finite difference method. In fact, by the Taylor expansion

$$N(T + \Delta T) = N(T) + \frac{dN(T)}{dT}\Delta T + \frac{d^2N(T)}{dT^2}(\Delta T)^2 + o((\Delta T)^2)$$

Neglecting the high-order terms $o((\Delta T)^2)$, we have

$$\frac{N(T + \Delta T) - N(T)}{\Delta T} = \frac{dN(T)}{dT} + \frac{d^2N(T)}{dT^2}\Delta T$$

Hence, the finite difference method introduces

$$f_{III}(T) = -\frac{d^2N(T)}{dT^2}\Delta T \tag{A8}$$

Recall that $N(T) = \exp(TA) N_0$, so

$$\frac{d^2N(T)}{dT^2} = \frac{d^2}{dT^2}[\exp(TA) N_0] = A^2 \exp(TA) N_0$$

Therefore, the error term in Eq. A7 is given by

$$\begin{aligned}&\exp(TA) \int_0^T \exp(-sA) f_{III}(s) ds \\ &\quad = -\exp(TA) \int_0^T \exp(-sA) A^2 \exp(sA) N_0 \Delta T ds \\ &\quad = -A^2 \exp(TA) N_0 \Delta T T\end{aligned}$$

Notice that

$$A = V\begin{pmatrix} \lambda_1 & 0 \\ 0 & \lambda_2 \end{pmatrix} V^{-1}$$

where the columns of the matrix V are the eigenvectors of the matrix A associated with its eigenvalues λ_1 and λ_2, which are given by

$$\lambda_1 = 0 \qquad \text{and} \qquad \lambda_2 = -(k_{f-s} + k_{s-f})$$

and V^{-1} is the inverse of the matrix V. By definition

$$\begin{aligned} \exp(TA) &= \sum_{n=0}^{\infty} \frac{(TA)^n}{n!} = \sum_{n=0}^{\infty} \frac{T^n}{n!} A^n \\ &= \sum_{n=0}^{\infty} \frac{T^n}{n!} \left[V\begin{pmatrix} \lambda_1 & 0 \\ 0 & \lambda_2 \end{pmatrix} V^{-1} \right]^n \\ &= V\left\{ \sum_{n=0}^{\infty} \frac{T^n}{n!} \begin{bmatrix} (\lambda_1)^n & 0 \\ 0 & (\lambda_2)^n \end{bmatrix} \right\} V^{-1} \\ &= V\begin{Bmatrix} \exp(\lambda_1 T) & 0 \\ 0 & \exp(\lambda_2 T) \end{Bmatrix} V^{-1} \end{aligned}$$

Therefore, the error term in Eq. A7 becomes

$$\begin{aligned} &-\left[V\begin{pmatrix} 0 & 0 \\ 0 & \lambda_2 \end{pmatrix} V^{-1} \right]^2 \left[V\begin{pmatrix} 0 & 0 \\ 0 & \exp(\lambda_2 T) \end{pmatrix} V^{-1} \right] N_0 \Delta TT \\ &\quad = -V\begin{bmatrix} 0 & 0 \\ 0 & (\lambda_2)^2 \exp(\lambda_2 T) \end{bmatrix} V^{-1} N_0 \Delta TT \\ &\quad = T\exp(\lambda_2 T)\boldsymbol{c} = T\exp[-(k_{f-s} + k_{s-f})T]\boldsymbol{c} \end{aligned}$$

where $\boldsymbol{c}$ is a vector. Finally, by substituting $\exp(TA)N_0 = \boldsymbol{c}_1 + \boldsymbol{c}_2 \exp[-(k_{f-s} + k_{s-f})T]$ into Eq. A7, we obtain the leading and dominant terms of $N_{III}(T)$

$$\boldsymbol{c}_1 + \boldsymbol{c}_2 \exp[-(k_{f-s} + k_{s-f})T] + \boldsymbol{c}_3 T \exp(c_4 T) \quad \text{(A9)}$$

The solutions in Eqs. A3, A6, and A9 lead to Eqs. 26a and 26b or 27a and 27b corresponding to the initial conditions (i) or (ii), respectively.

Manuscript received May 6, 1996, and revision received May 27, 1998.